Non-line-of-Sight Optical Positioning Under Full-Duplex Ultraviolet Communication Scenarios

Gang Liu, Siming Wang, Renzhi Yuan, Mugen Peng.
State Key Laboratory of Networking and Switching Technology,
Beijing University of Posts and Telecommunications, Beijing, 100876, China
e-mails: {rothony, wangsiming, renzhi.yuan, pmg}@bupt.edu.cn

***Abstract*—Determining the position of non-line-of-sight (NLOS) targets using traditional optical positioning methods remains a challenge. Recently, a NLOS optical positioning method using ultraviolet (UV) signals was proposed to enhance the single-scattering links of UV communications. Practical UV communication suffers from low achievable information rate due to the wide pulse spreading effect caused by strong scattering. Full-duplex techniques can be employed to improve the achievable information rate. However, full-duplex techniques introduce severe self-interference (SI) to transmitters of UV communications, which will inevitably degrade the performance of NLOS optical positioning. In this work, we propose a NLOS optical positioning method for full-duplex ultraviolet communications. To mitigate the influence of SI, we first approximate the path loss of the SI as a Fourier series (FS), then subtract the SI from the receiving power for calculating the location and pointing angles of the transmitter. Numerical results indicate that the proposed FS can will approximate the SI calculated from Monte-Carlo simulation models. Besides, we found that the proposed NLOS UV positioning method for full-duplex UV communications can achieve a positioning error of less than 3 meters and an azimuth error of less than 1.2 degrees within typical transceiver geometries up to 100 meters, significantly improving performance compared to positioning under scenarios with unresolved SI.**

***Index Terms*—Full-duplex, non-line-of-sight, self-interference mitigation, ultraviolet positioning**

I. Introduction

Ultraviolet (UV) communication utilizes the solar-blind band ($200 \sim 280$ nm) light for information transmission, characterized by low background noise and enhanced secrecy [1]. Unlike traditional optical communication, UV communication can leverage atmospheric particles for scattering, thereby enabling non-line-of-sight (NLOS) communication [2]–[4]. These advantages render UV light communication extensively applicable in military settings, indoor scenarios, and electromagnetic-sensitive environments.

Traditional optical positioning technologies rely on LOS links, limiting their application [5]. However, the NLOS characteristic of UV light broadens the possibilities for positioning [6]. Beyond merely acquiring the precise location of target, UV light positioning can also facilitate communication, achieving higher communication efficiency and precision. Specifically, when the receiver is aware of the geometric parameters of the transmitter, such as position and orientation, it can dynamically adjust its own parameters to establish a more stable communication link, thereby enhancing communication performance.

Current research on UV light positioning mainly focuses on simplex communication scenarios. Some works centered on UV light networks by using ranging algorithms to determine the distance between the receiver and the target upon knowing the received power, where multi-node positioning algorithms are employed to pinpoint the coordinates of the target [7], [8]. However, this requires prior knowledge of the precise locations of all receivers in the network. Single-user positioning methods were initially proposed in neighbor discovery protocols for UV ad-hoc networks [9]–[12]. Nonetheless, these approaches are somewhat limited in application, providing only partial information such as the communication direction, and they struggle to ascertain the location of target. Recently, a NLOS positioning method based on two photon-counting receivers to compute the distance and azimuth of the target was proposed [13], and was extended to multiple linearly-arrayed receivers [14]. However, the impact of full-duplex communication was not considered.

NLOS UV communication suffers from low information transmission rates due to the wide pulse spreading effect caused by strong scattering. Full-duplex UV communications can be used to improve the achievable information transmission rates [15]–[18]. However, since UV light transmission relies on atmospheric particles for scattering, receivers in full-duplex UV communication are subjected to strong self-interference (SI) from their own transmitters, which significantly reduces the system performance. Therefore, it is necessary to study how to mitigate the effects of SI in a full-duplex scenario to achieve NLOS UV positioning.

In this work, we propose a method for mitigating SI in a full-duplex scenario for NLOS UV positioning, in order to determine the location and orientation of the target user. We first simulate the SI using a Monte Carlo multiple

This work is supported by the National Key Research and Development Program of China under Grant 2021YFB2900200, National Natural Science Foundation of China under No. 62201075 and 61925101, the Beijing Natural Science Foundation under Grant L223007, and the Beijing Municipal Science and Technology Project NO. Z211100004421017.

Corresponding author: Renzhi Yuan.

scattering integration model [19], [20], and then propose a Fourier series (FS) exponential function to fit the SI. To calculate the position and orientation angle of the target user, we subtract the SI from the received power and following the NLOS positioning method proposed in [13]. Numerical results show that the FS exponential can well approximate the SI calculated by the Monte Carlo simulation model. Besides, the proposed NLOS optical positioning method under SI can achieve a positioning error of less than 3 meters in distance and less than 1.2° in azimuth within a range of 100 meters. In addition, we also find that mitigating SI can significantly improve the accuracy of distance positioning and the elevation angle of the target user.

II. NLOS UV Positioning Method Under Self-Interfernce

The main purpose of full-duplex UV positioning is to obtain the location of the target user and its pointing of the transmitted beam. A typical scenario of NLOS UV positioning under SI in a full-duplex communication scenario is shown in Figure 1, Where user 1 is located at the origin of the coordinate system $C(x, y, z)$; l_T is the axis of the transmitted light beam of user 2, with the direction vector μ_T; l_i is the axis of the receiving field of view (FOV) of user 1 intersecting with l_T under the elevation angle θ_i, with the direction vector μ_i, where $i \in 1, 2$; l_I is the axis of the transmitted light beam of user 1, with the direction vector μ_I; l is the line between users 1 and 2, with the direction vector μ_l; ϕ_l is the angle between line l and the x-axis; r is the distance between users 1 and 2. To obtain the coordinates of transmitter on the horizontal plane H, it is necessary to determine the azimuth angle ϕ_l of line l and the distance r between the users.

Given the symmetry inherent in full-duplex UV communication, for simplicity, we consider a scenario where only user 2 transmits signals, and user 1 receives signals while being subject to interference from its own transmitter. Without loss of generality, we restrict the positioning problem to a two-dimensional scenario, assuming that users 1 and 2 are located on the same horizontal plane H. When both users in the duplex communication system employ the same system design, it is reasonable to assume that user 1 knows the transmit power P_t of the transmitter of user 2, and the divergence angle β_t of the transmit beam.

The proposed UV positioning method can be divided into two steps. In section II-A, we simulate the SI using the Monte Carlo multiple scattering integration model, then fit the SI using a FS exponential model. In section II-B, we determine the position and orientation of the target user.

A. Approximation Model for SI in Full-Duplex UV Communications

The presence of SI severely affects the signal detection at the receiver of user 1, making it necessary to approximate the magnitude of SI by modeling the SI as an analytical form. The intensity of UV scattering decreases significantly with increasing orders of scattering, with the intensity of first-order scattering being much greater than that of higher-order scattering. Therefore, the communication link between User 1 and User 2 relies on first-order UV scattering. When the axis of the SI beam of user 1 intersects with the FOV, the first-order scattering becomes the main component of SI. In this case, the SI is much greater than that of the useful signals because the distance between the transmitter and receiver of the SI link is much smaller than the distance between Users 1 and 2. Therefore, it is necessary to impose the restriction on the transceiver geometry to ensure the absence of first-order scattering signals in SI. We suppose the transmitter is located in the middle of the device and can rotate up and down; the device has two bases at the top and bottom, which can mount receivers that can rotate 360 degrees. The receivers can be freely disassembled and installed on the two bases and can also rotate up and down. Then, to avoid the intersection between the transmitting and receiving fields of view of the user, the elevation angle θ_I of the transmitting beam should satisfy

$$\theta_I \in \left[\theta_1 + \frac{\beta_t + \beta_r}{2}, \theta_2 - \frac{\beta_t + \beta_r}{2}\right], \tag{1}$$

where θ_1 and θ_2 are the elevation angles of the receiver at the lower and upper bases, respectively, β_t is the divergence angle of the transmitter, and β_r is the divergence angle of the receiver. At this point, the SI is composed only of higher-order scattering signals [21], and the received signals are primarily composed of the transmitted signals of the opponent, ensuring normal positioning operations. For the intensity of higher-order scattering signals, we use a Monte Carlo multiple scattering integration model to simulate the SI [19]. We fix the elevation and azimuth angles of the transmitter, the elevation angle of the receiver, and the distance between the transmitter and receiver, and rotate the receiver to obtain the SI power at different receiver azimuth angles. We then use a FS to fit the logarithm of SI power as

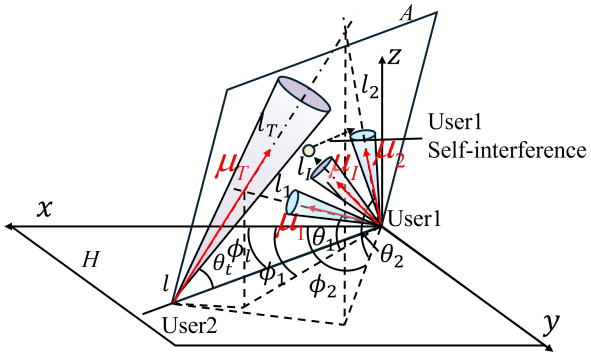

Fig. 1. Scenario of NLOS optical positioning under SI

follows:

$$P_I(\phi) = 10^{a_0+\sum_{n=1}^{N}[a_n\cos(\omega n\phi)+b_n\sin(\omega n\phi)]}, \tag{2}$$

where ϕ is the azimuth angle difference between the receiver and transmitter, a_0, a_n, and b_n are fitting parameters dependent on the elevation angle difference θ, and N is the order of the fitted FS.

B. NLOS Optical Positioning Method Under Full-Duplex UV Communications

The key to obtaining the azimuth angle ϕ_l lies on using the received power $P_{R,1}$ and $P_{R,2}$ to identify the two intersecting receiving FOV axes, l_1 and l_2, with the transmitted beam axis l_T, where $P_{R,i}$ for $i \in \{1,2\}$ is defined as the power received under the elevation angle θ_i for the ith receiving elevation angle. The received power in UV communication encompasses not only the signal power emitted by user 2 but also the SI power generated by the transmitter of user 1. Therefore, $P_{R,i}$ consists of both the signal power $P_{S,i}$ and the SI power $P_{I,i}$, following the relationship $P_{R,i} \triangleq P_{S,i} + P_{I,i}$.

By fixing the elevation angle θ_i and rotating the receiver of user 1 around the z axis, $P_{S,i}$ reaches its maximum when the transmitted beam axis of user 2 and the receiving FOV axis of user 1 intersect with each other. It is crucial to ascertain the received power $P_{R,i}$ and the SI power $P_{I,i}$ at different azimuth reception angles.

The photon-counting receiver can obtain the average receiving power $P_{R,i}^m$ by estimating the average number of photons as

$$\hat{P}_{R,i}^m = \frac{\lambda_{s,i} h\nu}{T_d}, \tag{3}$$

where h is the plank constant; ν is the frequency of the transmitted UV light; $\lambda_{s,i}$ is the average number of photons, which can be obtained by averaging the number of received photons in K bit intervals according to the law of large numbers, i.e.,

$$\lambda_{s,i} = \frac{1}{M}\sum_{m=1}^{K} n_m, \tag{4}$$

where n_m is the detected number of photon at the mth bit interval satisfying the Poisson distribution with parameter $\lambda_{s,i}$, i.e.,

$$p(n_i) = \frac{\lambda_{s,i}^{n_i}}{n_i!} e^{-\lambda_{s,i}}. \tag{5}$$

When user 1 rotates around the z axis at an elevation angle θ_i, the received powers $P_{R,i}^1, P_{R,i}^2, \cdots, P_{R,i}^M$ are measured at M azimuth angles $\phi^1, \phi^2, \cdots, \phi^M$. The maximum signal power $P_{S,i}^{max}$ and its corresponding azimuth angle ϕ_i can be obtained by using the calculated $P_{R,i}(\phi)$ and the fitted $P_{I,i}(\phi)$

$$\begin{cases} P_{S,i}^{max} = \max\{P_{R,i}^1(\phi^1) - P_{I,i}^1(\phi^1), P_{R,i}^2(\phi^2) - P_{I,i}^2(\phi^2), \\ \cdots, P_{R,i}^M(\phi^M) - P_{I,i}^M(\phi^M)\} \\ \phi_i = \underset{\{\phi^1,\cdots,\phi^M\}}{\arg\max}\ \{P_{S,i}^1(\phi^1), P_{S,i}^2(\phi^2), \cdots, P_{S,i}^M(\phi^M)\}. \end{cases} \tag{6}$$

According to (6), the estimated $\hat{\phi}_i$ is obtained as the corresponding azimuth angle of $\hat{P}_{S,i}$. In practical implementations, the receiving azimuth angle is directly read by a protractor or a goniometer; and thus the distribution of $\hat{\phi}_i$ is closely related to the employed instruments. For simplicity, we assume that the receiving azimuth angle $\hat{\phi}_i$ satisfies a Gaussian distribution with mean ϕ_i and variance $\sigma_{\phi_{R,i}}^2$.

Using the maximum signal power, we can get the two lines l_1 and l_2 that intersect l_T. Denoting the elevation and azimuth angles of $l_{(1)}$ and $l_{(2)}$ by $\theta_{(1(2))}$ and $\phi_{(1(2))}$, respectively, the direction vectors of l_1 and l_2 can be obtained as

$$\begin{cases} \boldsymbol{\mu}_1 = [\cos\theta_1\cos\phi_1, \cos\theta_1\sin\phi_1, \sin\theta_1]^{\mathrm{T}} \\ \boldsymbol{\mu}_2 = [\cos\theta_2\cos\phi_2, \cos\theta_2\sin\phi_2, \sin\theta_2]^{\mathrm{T}}. \end{cases} \tag{7}$$

From [13], the expression of the azimuth angle ϕ_l can be obtained as follows:

$$\phi_l = \arctan\left(-\frac{a}{b}\right) + k\pi, \tag{8}$$

where $k \in \mathbb{Z}$. When ϕ_l is restricted in $[0, 2\pi]$, there are two azimuth angle ϕ_l^1 and ϕ_l^2 satisfy (8), which are at inverse directions because $|\phi_l^1 - \phi_l^2| = \pi$. Nevertheless, we choose the one with larger receiving power, which corresponds to the one with $\boldsymbol{\mu}_{R,i} \cdot \boldsymbol{\mu}_l > 0$, and where $\boldsymbol{\mu}_l \triangleq [\cos\phi_l, \sin\phi_l, 0]^{\mathrm{T}}$ is the direction vector of ray l.The coefficients a and b in the azimuth angle formula are defined by the relations:

$$\begin{cases} a = -\cos\theta_1\sin\phi_1\sin\theta_2 + \cos\theta_2\sin\phi_2\sin\theta_1 \\ b = \cos\theta_1\cos\phi_1\sin\theta_2 - \cos\theta_2\cos\phi_2\sin\theta_1. \end{cases} \tag{9}$$

We consider the coplanar situation on plane A, which allows for the determination of the angles $\theta_{r,1}$ and $\theta_{r,2}$ formed between the lines l_1, l_2, and the line l within plane A. Then we have

$$\begin{cases} \theta_{r,1} = \arccos\left(\cos\theta_1\cos\left(\phi_1 - \phi_l\right)\right) \\ \theta_{r,2} = \arccos\left(\cos\theta_2\cos\left(\phi_2 - \phi_l\right)\right). \end{cases} \tag{10}$$

In the calculation of the azimuth angle ϕ_l, the maximum received signal powers when the receiver points towards μ_1 and μ_2, denoted as $P_{S,1}^{max}$ and $P_{S,2}^{max}$, are known.These can be used to further solve for the transmitter-receiver distance using the NLOS scattering channel model. In short-distance communication scenarios, using a single scattering model [22]–[25], the received power can be expressed as an analytic expression $P_S(r, \theta_t, \theta_r)$ concerning the distance between transmitter and receiver r, and the coplanar elevation angles θ_r, θ_s [22], as shown in Fig. 2.

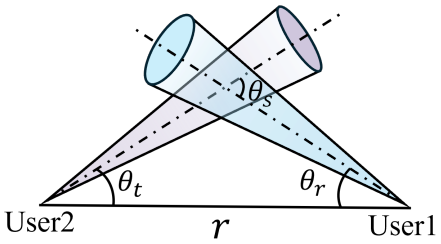

Fig. 2. Coplanar single-scattering model of UV communication system

Within plane A, given $\theta_{r,1}$, $\theta_{r,2}$, and θ_t, the distance r between the users can be calculated by solving the following equation

$$\begin{cases} P_s(r,\theta_t,\theta_{r,1}) = P_{S,1}^{max} \\ P_s(r,\theta_t,\theta_{r,2}) = P_{S,2}^{max}, \end{cases} \tag{11}$$

where θ_t represents the angle between the transmission axis and l; $\theta_{r,1}$ and $\theta_{r,2}$ represent the coplanar elevation angles of the receiver. The equations in (11) can be solved by finding the solution to the following optimization problem:

$$\begin{aligned} \left\{\hat{r},\hat{\theta}_t\right\} = \arg\min_{\{r,\theta_t\}} & \sqrt{\sum_{i=1}^{2}\left[P_s\left(r,\theta_t,\theta_{r,i}\right)-P_i\right]^2} \\ \text{s.t.} & 0<r<r_{max} \\ & 0<\theta_t<\pi, \end{aligned} \tag{12}$$

where r_{max} is the maximum distance.

After obtaining θ_t, we can obtain the pointing angles θ_T, ϕ_T of the transmitter as

$$\begin{cases} \theta_T = \arcsin(|\sin\theta_t\sqrt{1-(\cos\theta_1\cos\theta_2\sin(\phi_1-\phi_2))^2}|) \\ \phi_T = \phi_r + \arccos\left(\frac{\cos\theta_t}{\cos\theta_T}\right) + k\pi, \end{cases} \tag{13}$$

where $k \in \mathbb{Z}$. When ϕ_r is restricted in $[0, 2\pi]$, there are two azimuth angle $\phi_{T,1}$ and $\phi_{T,2}$ satisfying with $|\phi_{T,1}-\phi_{T,2}| = \pi$. Nevertheless, we choose the one with smaller $|\vec{\mu}_T \cdot \vec{\mu}_A|$.

C. Sampling of Receiving Powers and Receiving Azimuth Angles

The positioning error and pointing error can be represented by the standard deviation of $\{r, \phi_l, \theta_T, \phi_T\}$. We can use the Monte Carlo methods to obtain the root-mean-square error (RMSE) of the estimated r, ϕ_l, θ_T, and ϕ_T. The Monte Carlo method first samples the receiving azimuth angles ϕ_1 and ϕ_2 to obtain ϕ_l, then samples the maximum receiving power $P_{S,1}$ and $P_{S,2}$ to obtain the distance r, θ_T, and ϕ_T. As we mentioned in Section II-B, the receiving azimuth angle satisfies a Gaussian distribution with expectation $\phi_{R,i}$ and standard deviation σ_{ϕ_i}. The standard deviation σ_{ϕ_i} is related to the employed measuring instrument. Without loss of generality, we set $\sigma_{\phi_i} = 1$ in this paper. The theoretical receiving azimuth angle ϕ_i can be expressed as

$$\phi_i = \phi_l + \arcsin\left(\frac{\tan\theta_i}{\tan\theta_T}\sin\left(\phi_T-\phi_l\right)\right). \tag{14}$$

Then the receiving azimuth angles can be sampled by

$$\hat{\phi}_i = normrnd(\phi_i, \sigma_{\phi_i}), \tag{15}$$

where $normrnd(\mu, \sigma)$ generates a random number satisfying Gaussian distribution with mean μ and variance σ^2.

Then after obtaining the ϕ_i, we can obtain $\theta_{r,i}$ by (10). The elevation angle θ_t of the transmitter in plane α can be obtained as

$$\theta_t = \arccos\left(-\cos\theta_T\cos\left(\phi_T-\phi_l\right)\right). \tag{16}$$

Then the theoretical maximum receiving power $P_{R,i}$ for the ith receiver can be obtained by substituting r, θ_t and $\theta_{r,i}$ into the analytical average receiving power function $P_S\left(r,\theta_t,\theta_r\right)$.

Then the expectation of the receiving photon numbers can be obtained as $\lambda_{s,i} = \frac{P_{R,i}T_d}{h\nu}$. Then the maximum receiving power can be sampled by

$$\hat{P}_{R_i} = \frac{poissrnd(\lambda_{s,i})h\nu}{T_d}, \tag{17}$$

where $poissrnd(\lambda_s)$ generates a random number satisfying Poisson distribution with mean value of λ_s.

III. Numerical Results

In this section, we provide some numerical results to explore the performance of the proposed UV positioning method. Unless otherwise specified, the simulation parameters are given in Table I. Besides, the positioning errors are represented by the RMSE of the estimated ϕ_l, r, θ_T, and ϕ_T, where the RMSE are obtained by running 10^4 trials of the Monte Carlo method.

TABLE I
Simulation Parameters

Parameter	Value	Parameter	Value
r	$50\,\mathrm{m}$	ϕ_l	$0°$
θ_T	$45°$	ϕ_T	$180°$
θ_I	$45°$	c	$2.998\times10^8\,\mathrm{m\,s^{-1}}$
$\theta_{R,1}$	$20°$	$\theta_{R,2}$	$70°$
β_t	$17°$	β_r	$20°$
P_t	$500\,\mathrm{mW}$	A_r	$1.77\times10^{-4}\,\mathrm{m^2}$
T_d	$1\times10^{-5}\,\mathrm{s}$	k_a	$0.802\,\mathrm{km^{-1}}$
k_s^{Ray}	$0.266\,\mathrm{km^{-1}}$	k_s^{Mie}	$0.284\,\mathrm{km^{-1}}$
γ	0.017	g	0.72
f	0.5	h	$6.626\times10^{-34}\,\mathrm{J\,s}$

A. Approximation of SI

Due to the relatively small magnitude of SI power, we first perform a logarithmic transformation of the SI power for convenience in handling. To ensure that the fitting function accurately captures periodic patterns, we have expanded the

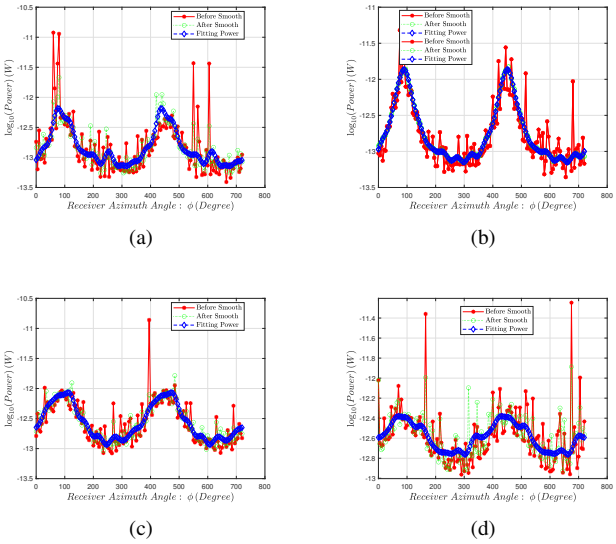

Fig. 3. The magnitude of SI power and the corresponding fitting curve at different receiver elevation angles: (a) receiver elevation angle of 10°;(b) receiver elevation angle of 20°;(c) receiver elevation angle of 70°;(d) receiver elevation angle of 80°.

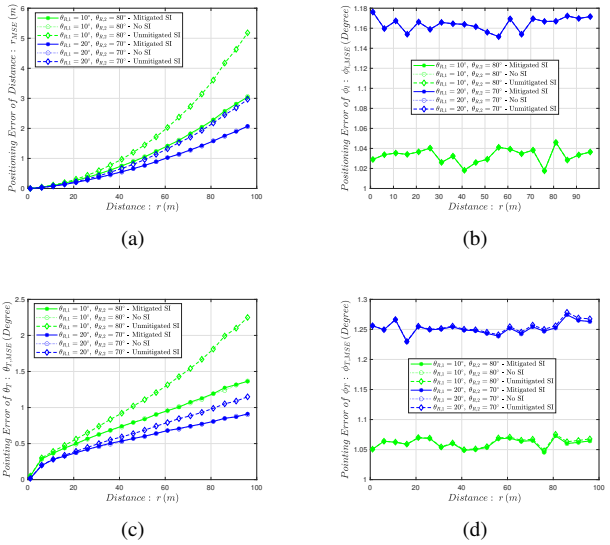

Fig. 4. Pointing error of parameters under different r,different situations and elevation angle (θ_1, θ_2): (a) Pointing error of r under different r; (b) Pointing error of ϕ_l under different r; (c) Pointing error of θ_T under different r; (d) Pointing error of ϕ_T under different r.

SI power data. The specific method is to copy the SI power from 0 to 360 degrees in the original data and append it from 361 degrees to 722 degrees, thus forming a periodic new dataset. Considering the randomness of Monte Carlo simulations, the original data contains much noise. To reduce this noise, we have smoothed the data. Finally, the data fitting was carried out using the method described in 2. For the order N of the FS, the higher the order, the better the accuracy of the fit, but the corresponding computation also increases. In this study, $N = 8$ was chosen as the order of the FS. As shown in Fig. 3, the noise in the SI power data significantly reduced after smoothing. Using an 8th order FS fitting function, the RMSE at $\theta = 10°, 20°, 70°, 80°$ reached errors of 0.14, 0.019, 0.09, and 0.13 respectively, all showing high fitting accuracy, indicating that our proposed FS exponential fitting can well fit the SI power obtained from Monte Carlo multiple scattering integration model.

B. Positioning Performance

We present the RMSE of different parameters under varying distance r, different scenarios, and elevation angles $(\theta_1, \theta_2) \in (20°, 70°), (10°, 80°)$, as shown in Fig. 4. Here, "NO SI" indicates a simplex communication system without SI, "Unmitigated SI" refers to a duplex communication system with SI unmitigated, and "Mitigated SI" indicates a duplex communication system where SI has been mitigated.

Fig. 4(a) shows the RMSE of r varies under different r, different scenarios, and elevation angles (θ_1, θ_2). We find that the error in distance r increases with the increase in r. With our proposed method for mitigating SI in NLOS UV positioning, the positioning error in distance r in a duplex system can be nearly identical to that of a simplex system, and significantly less than that in scenarios where SI is not mitigated. At an elevation angle of $(10°, 80°)$, the positioning error in distance r can be less than 3 meters when SI is mitigated, showing a precision improvement of up to 2 meters compared to when it is unmitigated; at an elevation angle of $(20°, 70°)$, the error can be about 2 meters, with an improvement of up to 1 meter compared to unmitigated scenarios.

Fig. 4(b) shows the RMSE of ϕ_l under different r, different situations, and elevation angles (θ_1, θ_2). We find that ϕ_l is unaffected by distance r or the different scenarios. As indicated by (8), ϕ_l is not determined by r or power but solely by μ_1, μ_2. Furthermore, our proposed method for mitigating SI in NLOS UV positioning can achieve an azimuthal error of less than 1.2 degrees within 100 meters.

Fig. 4(c) shows the RMSE of θ_T under different r, different situations, and elevation angles (θ_1, θ_2). We observe that the error in elevation angle θ_T increases with the distance r. With our proposed method, the error in θ_T in a duplex system can be nearly identical to that of a simplex system and is significantly less than in scenarios where SI is not mitigated. At an elevation angle of $(10°, 80°)$, the error in θ_T can be less than $1.5°$ when SI is mitigated, showing a precision improvement of nearly 1 degree; at $(20°, 70°)$, the error can be about $0.8°$, with an improvement of approximately $0.3°$.

Fig. 4(d) shows the RMSE of ϕ_T under different r, different scenarios, and elevation angles (θ_1, θ_2). We find that the error in ϕ_T fluctuates slightly with changes in distance but remains generally constant. When the interval between elevation angles increases, the error in ϕ_T decreases.

Furthermore, the impact of considering and mitigating SI on ϕ_T is almost negligible. At an elevation angle of $(10°, 80°)$, the error in ϕ_T is about $1.25°$; at $(20°, 70°)$, it is about $1.05°$.

IV. Conclusion

In this work, we have proposed a method for mitigating SI in a duplex communication scenario for NLOS UV positioning. Numerical results show that the FS exponential can well approximate the SI calculated by the Monte Carlo simulation model, and the proposed NLOS optical positioning method under SI can achieve a positioning error of less than 3 meters in distance and less than $1.2°$ in azimuth within 100 meters. Additionally, we found that mitigating SI significantly improves the accuracy of distance and elevation angle positioning for the target user.

References

[1] A. Vavoulas, H. G. Sandalidis, N. D. Chatzidiamantis, Z. Xu, and G. K. Karagiannidis, "A Survey on Ultraviolet C-Band (UV-C) Communications," *IEEE Commun. Surv. Tutor.*, vol. 21, no. 3, pp. 2111–2133, Feb. 2019.

[2] R. Yuan and J. Ma, "Review of ultraviolet non-line-of-sight communication," *China Commun.*, vol. 13, no. 6, pp. 63–75, June 2016.

[3] R. Yuan and M. Peng, "Single-input multiple-output scattering based optical communications using statical combining in turbulent channels," *IEEE Trans. Wirel. Commun.*, vol. 23, no. 4, pp. 2560–2574, Aug. 2023.

[4] S. Wang, M. Peng, and R. Yuan, "Mimo free-space optical communications using photon-counting receivers under weak links," *IEEE Commun. Lett.*, vol. 27, no. 4, pp. 1185–1189, 2023.

[5] H. Li, H. Huang, Y. Xu, Z. Wei, S. Yuan, P. Lin, H. Wu, W. Lei, J. Fang, and Z. Chen, "A fast and high-accuracy real-time visible light positioning system based on single led lamp with a beacon," *IEEE Photonics J.*, vol. 12, no. 6, pp. 1–12, Dec. 2020.

[6] Q. Zhang, X. Zhang, L. Wang, G. Shi, Q. Fu, and T. Liu, "Performance modeling of ultraviolet atmospheric scattering of different light sources based on monte carlo method," *Appl. Sci.*, vol. 10, p. 3564, May. 2020.

[7] T. Zhao, X. Yu, P. Liu, and L. Liu, "Ultraviolet anti-collision and localization algorithm in uav formation network," *Optik*, vol. 192, p. 162919, Sep. 2019.

[8] L. Guo, Y. Guo, J. Wang, and T. Wei, "Ultraviolet communication technique and its application," *J. Semicond.*, vol. 42, no. 8, p. 081801, aug 2021.

[9] Y. Li, L. Wang, Z. Xu, and S. V. Krishnamurthy, "Neighbor discovery for ultraviolet ad hoc networks," *IEEE J. Sel. Areas Commun.*, vol. 29, no. 10, pp. 2002–2011, Dec 2011.

[10] H. Qi, C. Gong, and Z. Xu, "Omnidirectional antenna array-based transmitter direction sensing in ultra-violet ad-hoc scattering communication networks," in *IEEE Int. Conf. Commun. Workshops*, May 2019, pp. 1–6.

[11] L. Wang, Y. Li, Z. Xu, and S. V. Krishnamurthy, "A novel neighbor discovery protocol for ultraviolet wireless networks," in *Proc. ACM Int. Conf. Model. Anal. Simul. Wirel. Mob. Syst.*, 2011, pp. 135–142.

[12] Y. Zhao, Y. Zuo, H. Qin, X. Zhang, Q. An, and J. Wu, "A neighbor discovery protocol in ultraviolet wireless networks," in *Asia Commun. Photonics Conf.*, Nov 2014, pp. 1–3.

[13] S. Wang, R. Yuan, M. Peng, Z. Wang, X. Chu, S. Di, K. Sun, and D. Zhang, "Non-line-of-sight ultraviolet positioning using two photon-counting receivers," in *GLOBECOM 2023*, Dec. 2023, pp. 3682–3687.

[14] R. Yuan, S. Wang, G. Liu, and M. Peng, "Non-line-of-sight ultraviolet positioning using linearly-arrayed photon-counting receivers," *IEEE J. Sel. Areas Commun.*, Early Access 2024.

[15] Z. Zhang, K. Long, A. V. Vasilakos, and L. Hanzo, "Full-duplex wireless communications: Challenges, solutions, and future research directions," *Proc IEEE Inst. Electr. Electron. Eng.*, vol. 104, no. 7, pp. 1369–1409, July 2016.

[16] Z. Wang, R. Yuan, and M. Peng, "Non-line-of-sight full-duplex ultraviolet communications under self-interference," *IEEE Trans. Wirel. Commun.*, vol. 22, no. 11, pp. 7775–7788, Nov 2023.

[17] Z. Wang, R. Yuan, J. Cheng, and M. Peng, "Joint optimization of full-duplex relay placement and transmit power for multihop ultraviolet communications," *IEEE Internet Things J.*, vol. 11, no. 7, pp. 11 960–11 973, April 2024.

[18] Z. Wang, R. Yuan, M. Peng, S. Wang, X. Chu, and S. Di, "Full-duplex relay for ultraviolet communications using photomultiplier tube receivers," in *2023 IEEE/CIC Int. Conf. Commun. China*, Aug 2023, pp. 1–6.

[19] R. Yuan, J. Ma, P. Su, Y. Dong, and J. Cheng, "Monte-carlo integration models for multiple scattering based optical wireless communication," *IEEE Trans. Commun.*, vol. 68, no. 1, pp. 334–348, Jan 2020.

[20] ——, "An importance sampling method for monte-carlo integration model for ultraviolet communication," in *2019 International Conference on Advanced Communication Technologies and Networking (CommNet)*. IEEE, 2019, pp. 1–6.

[21] R. Yuan, J. Ma, P. Su, and Z. He, "An integral model of two-order and three-order scattering for non-line-of-sight ultraviolet communication in a narrow beam case," *IEEE Commun. Lett.*, vol. 20, no. 12, pp. 2366–2369, 2016.

[22] Z. Xu, H. Ding, B. M. Sadler, and G. Chen, "Analytical performance study of solar blind non-line-of-sight ultraviolet short-range communication links," *Opt. Lett.*, vol. 33, no. 16, pp. 1860–1862, Aug. 2008.

[23] T. Wu, J. Ma, P. Su, R. Yuan, and J. Cheng, "Modeling of short-range ultraviolet communication channel based on spherical coordinate system," *IEEE Commun. Lett.*, vol. 23, no. 2, pp. 242–245, 2019.

[24] T. Wu, J. Ma, R. Yuan, P. Su, and J. Cheng, "Single-scatter model for short-range ultraviolet communication in a narrow beam case," *IEEE Photon. Technol. Lett.*, vol. 31, no. 3, pp. 265–268, 2019.

[25] X. Chu, R. Yuan, and M. Peng, "Turbulent single-scattering channel model for ultraviolet communications using equivalent scattering point approach," *IEEE Commun. Lett.*, Early Access 2024.